On the Cholesteric-Nematic Phase-Change Transition in Layers with Homeotropically Orienting Surfaces

Paul R. Gerber

Central Research Units, F. Hoffmann-La Roche & Co. Limited Company, Basel, Switzerland

Z. Naturforsch. **38 a**, 407–414 (1983); received November 8, 1982

Lattice-model calculations of the energies of surface director-configurations are presented. These configurations mediate between the homeotropic surface conditions and the bulk fingerprint texture of cholesteric layers. Their energy determines the asymptotic behaviour of the cholesteric-nematic threshold field in the limit of thick layers. The dependence of their energies on the elastic constant ratios could be brought into a simple scaling form. This form is in agreement with existing and newly presented measurements.

1. Introduction

The cholesteric-nematic phase-change transition in an applied magnetic field has been a subject of interest for some time. The first treatments which delt with the bulk situation gave a relatively transparent picture [1, 2]. However, the presence of surfaces led to a rich variety of additional effects the detailed understanding of which is still a matter of discussion. In particular there seems to be no consense on the detailed structure and energies of the director fields mediating between the boundary conditions imposed by the substrates and the bulk-like solution farther away. For the case of homeotropically aligning surfaces, to which we restrict ourselves in this work, planar director configurations have been proposed [3] which are to some extent treatable by analytical methods. Such configurations require the presence of singular lines or sheets in the director field and seem to disagree with experimental observations [3]. On the other hand disclination-free configurations (in the sense of non-singular) have been proposed which require a three-dimensional director field [4, 5].

The present investigation tries to obtain quantitative results for the disclination-free three-dimensional director field by numerical treatment of a lattice model. Furthermore, connection is made with measurable quantities, mainly with the thickness dependence of the threshold voltage. A knowledge of the mechanism governing this quantity is also of interest for possible application of the cholesteric-nematic transition in display technology [6, 9].

Reprint requests to Dr. P. R. Gerber, Central Research Units, F. Hoffmann-La Roche & Co. Limited Company, 4002 Basel, Schweiz.

2. General Considerations

The cholesteric-nematic phase-change transition in a bulk situation is of continuous (second order) type [1, 2]. The presence of homeotropically orienting surfaces changes this behaviour to a first order type transition [7, 8]. The following considerations quantify this finding to some extent.

2.1. Bulk solution

First we recapitulate the results of a consideration of the bulk case [1]. The applied magnetic field $\boldsymbol{H}$ is directed along the z-direction which causes the cholesteric helix axis to assume a perpendicular orientation, say along the x-direction. The free energy density of the director field $\boldsymbol{n}(\boldsymbol{r})$ reads [10]

$$F = \tfrac{1}{2}\{k_{11}(\operatorname{div}\boldsymbol{n})^2 + k_{22}(\boldsymbol{n}\cdot\operatorname{rot}\boldsymbol{n} + q_0)^2 + k_{33}(\boldsymbol{n}\times\operatorname{rot}\boldsymbol{n})^2 - \Delta\chi(\boldsymbol{n}\cdot\boldsymbol{H})^2\}, \quad (2.1)$$

where k_{11}, k_{22} and k_{33} are the elastic constants for splay-, twist- and bend deformation of the nematic director field $\boldsymbol{n}$, and $\Delta\chi$ is the anisotropy of the magnetic susceptibility taken to be positive in our case. The field-free pitch P_0 of the cholesteric is determined by the wave vector q_0 through

$$P_0 = \frac{2\pi}{q_0} \quad (2.2)$$

and corresponds to the distance along the helix axis over which the director has turned by an angle of 2π.

0340-4811 / 83 / 0400-0407 $ 01.3 0/0. – Please order a reprint rather than making your own copy.

In a field below the threshold value [1]

$$H_c = \frac{\pi^2}{P_0}\sqrt{k_{22}/\Delta\chi} \tag{2.3}$$

the unconstrained solution shows a periodicity in $\boldsymbol{n} = (0, \sin\psi(x), \cos\psi(x))$ of

$$P = q_H^{-1}\int_0^{2\pi} \mathrm{d}\psi (w - \cos^2\psi)^{-1/2}, \tag{2.4}$$

where $q_H^2 = \Delta\chi H^2/k_{22}$, and w is an integration parameter ($w \geqq 1$) obeying the equation

$$P_0^{-1} = \frac{1}{2}\pi^{-2}\int_0^{\pi}\frac{\mathrm{d}\psi}{\mathrm{d}x}\mathrm{d}\psi = \frac{q_H}{2\pi^2}\int_0^{\pi}\mathrm{d}\psi(w-\cos^2\psi)^{1/2}. \tag{2.5}$$

This solution has an averaged free energy density of

$$\bar{f} \equiv \frac{2}{P}\int_0^{\pi}\mathrm{d}\psi(F/k_{22} - \tfrac{1}{2}q_0^2)/\left(\frac{\mathrm{d}\psi}{\mathrm{d}x}\right) = -\tfrac{1}{2}q_H^2 w. \tag{2.6}$$

When the field H approaches H_c the parameter w goes from above towards the value $w_c = 1$. Eliminating w in this limit yields

$$1 - H/H_c \approx 4\left(\frac{\pi^2 P}{2P_0} + 1\right)\exp\left\{-\frac{\pi^2 P}{2P_0}\right\}, \tag{2.7}$$

showing that a pitch enlargement by a factor of two requires H to be only 2‰ below H_c. In other words, substantial changes in P take place only immediately below H_c.

2.2. *Influence of homeotropic surfaces*

The adaption of the bulk director configuration to the homeotropic boundary conditions requires the presence of a surface structure in the director field which mediates between the two topologically different situations. There have been several proposals for this structure such as a sequence of singular disclination lines [3] or disclination free possibilities [4, 5]. In any case such a structure has a higher energy than the bulk value given by (2.6) which applies for free boundary conditions. This incremental surface energy e_s is conveniently taken for one period P and per unit length in the direction y of translation invariance along the substrate. Clearly, e_s which in analogy to (2.6) is taken in units of k_{22}, depends on the elastic constant ratios

$$\sigma = \frac{k_{11}}{k_{22}} - 1, \qquad \tau = \frac{k_{33}}{k_{22}} - 1 \tag{2.8}$$

and also in general on P/P_0.

Let us assume for e_s a general asymptotic form

$$e_s \approx e_0(P/P_0)^{\lambda} \quad \text{as} \quad P \to \infty, \tag{2.9}$$

with a yet arbitrary exponent λ. The condition for the equilibrium between the homeotropic state and the fingerprint state is given by equalizing the difference between the energies of the homeotropic and fingerprint configuration for a layer of thickness d with twice the surface energy e_s, i.e.

$$2e_0(P_\gamma/P_0)^{\lambda} = q_{H,\gamma}^2(w_\gamma - 1)\,P_\gamma\,d/2, \tag{2.10}$$

where the subscript γ indicates the critical values appropriate to the equilibrium situation. For this equation to be valid, the spacing d must be large enough to exclude interactions between the opposite surface structures.

Taking the asymptotic form

$$w - 1 \approx 16\exp\left\{-\frac{\pi^2}{2}\frac{P}{P_0}\right\}$$

and $q_{H,\gamma} \to q_{H,c} = \pi^2/P_0$ as obtained from (2.4) and (2.5) one arrives from (2.10) at the critical condition

$$\frac{P_0}{d} \approx \frac{4\pi^4}{e_0}\left(\frac{P_\gamma}{P_0}\right)^{1-\lambda}\exp\left\{-\frac{\pi^2}{2}\frac{P_\gamma}{P_0}\right\}. \tag{2.12}$$

Elimination of P_γ/P_0 in favour of H_γ/H_c through (2.7) then yields

$$1 - H_\gamma/H_c \approx \frac{1}{2\pi^2}\frac{P_0}{d}e_0\left(\frac{2}{\pi^2}\ln\frac{d}{P_0}\right)^{\lambda}. \tag{2.13}$$

This expression gives essentially a linear asymptotic dependence of H_γ on P_0/d. The logarithmic corrections if present at all and the coefficient e_0 give indications on the energy of the surface structure. The simplest expectation regarding these disclination type director arrangements is that their energy approaches a constant non zero value in the limit $P \to \infty$. In the numerical work of the next section as well as in our experiments the values of P/P_0 remain always in a rather limited range which makes it very difficult to extract information on possible logarithmic correction to the P_0/d-dependence. Nevertheless information is easily extractable regarding the surface energies at the attainable values of H. In particular, their dependence on the elastic constant ratios (2.8) is a matter of some practical interest.

3. Numerical Calculations

3.1. Lattice model

For the following numerical calculation of the director field we introduced a lattice model which in the limit of vanishing lattice constant a matches onto the continuum equations. The substrate was taken parallel to the x-y-plane. For the free energy density F we took the following model

$$
\begin{aligned}
2\frac{a^2F}{k_{22}} &= q_0[(u_\uparrow+u)(v_\uparrow-v)-(v_\uparrow+v)(u_\uparrow-u)+(v_\rightarrow+v)(w_\rightarrow-w)-(w_\rightarrow+w)(v_\rightarrow-v)] \\
&\quad +(u_\rightarrow-u)^2+(u_\uparrow-u)^2+(v_\rightarrow-v)^2+(v_\uparrow-v)^2+(w_\rightarrow-w)^2+(w_\uparrow-w)^2 \\
&\quad +\sigma[(u_\rightarrow-u)^2+(w_\uparrow-w)^2+\tfrac{1}{2}(u_\rightarrow-u_\leftarrow)(w_\uparrow-w_\downarrow)] \\
&\quad +\tfrac{\tau}{4}\{(u_\rightarrow+u)^2[(u_\rightarrow-u)^2+(v_\rightarrow-v)^2+(w_\rightarrow-w)^2]+(w_\uparrow+w)^2[(u_\uparrow-u)^2+(v_\uparrow-v)^2+(w_\uparrow-w)^2] \\
&\quad +2uw[(u_\rightarrow-u_\leftarrow)(u_\uparrow-u_\downarrow)+(v_\rightarrow-v_\leftarrow)(v_\uparrow-v_\downarrow)+(w_\rightarrow-w_\leftarrow)(w_\uparrow-w_\downarrow)]\}-q_H^2w^2
\end{aligned}
\tag{3.1}
$$

in which u, v, w are the components of a unit vector at a given lattice site on a square lattice, while the subscript arrows pointing to the right or upwards indicate nearest-neighbour positions in positive x- and z-direction respectively. As natural in a lattice model, lengths (e.g. P, P_0, q_0^{-1} or q_H^{-1}) are taken as pure numbers. To convert to the dimensioned quantities of Sect. 2 they have to be multiplied by the lattice constant a.

A director configuration was then found by varying the directors n_l of the lattice until the total energy

$$E=\sum_l a^2F_l \tag{3.2}$$

reached a minimum.

The top-row directions were kept fixed, pointing upwards ($u=v=0$, $w=1$), to provide the homeotropic boundary condition of the substrate. In the bottom row the directors were kept fixed in directions corresponding to the bulk solution in the same external field. This case is described in the next section.

3.2 Bulk solution

In the bulk, translational invariance also holds along the z-direction, while the directors assume a planar orientation $u=0$, $v=\sin\psi$, $w=\cos\psi$. The free-energy density expression now reduces to

$$
\begin{aligned}
2\frac{a^2F}{k_{22}} &= 2q_0\sin(\psi-\psi_\rightarrow)+2-2\cos(\psi-\psi_\rightarrow) \\
&\quad -q_H^2\cos^2\psi\,.
\end{aligned}
\tag{3.3}
$$

Numbering the directors in the row by l and minimizing $\sum F_l$ with respect to the ψ_l yields the set of equations

$$
\begin{aligned}
\mu_l &= \frac{1}{2}\frac{\partial}{\partial\psi_l}\sum_m F_m \\
&= q_0[\cos(\psi_{l+1}-\psi_l)-\cos(\psi_l-\psi_{l-1})] \\
&\quad -\sin(\psi_{l+1}-\psi_l)+\sin(\psi_l-\psi_{l-1}) \\
&\quad +q_H^2\cos\psi_l\sin\psi_l=0, \quad -\infty<l<\infty\,.
\end{aligned}
\tag{3.4}
$$

Taking the average (denoted by the brackets $\langle\ \rangle$)

$$\langle\mu\rangle=\lim_{N\to\infty}\frac{1}{2N+1}\sum_{l=-N}^{N}\mu_l \tag{3.5}$$

shows that $\langle\cos\psi\sin\psi\rangle=0$.

The solutions can be characterised by the quantity

$$m=q_0\langle\cos(\psi_\rightarrow-\psi)\rangle-\langle\sin(\psi_\rightarrow-\psi)\rangle \tag{3.6}$$

giving the average torque passed on from site to site.

The periodicity in our calculations was fixed by the number of lattice sites L in a row. Upon applying a magnetic field the periodicity P of the bulk solution is altered with respect to the pitch P_0 of the cholesteric. Since we wanted to keep P fixed in our lattice we had to find the value of P_0 corresponding to the applied field.

This value depends on the particular choice of solution as characterized by m (3.6). As a very convenient choice we utilized the solutions obeying the condition

$$\frac{1}{P_0}=(2\pi)^{-2}\sum_{l=1}^{L}(\psi_l-\psi_{l-1})^2, \quad \psi_0=\psi_L-2\pi\,, \tag{3.7}$$

which matches onto the corresponding continuum condition (2.5) in the limit $L\to\infty$. In (3.7) P_0 is related to the parameter q_0 in (3.1) by

$$q_0=\tan\left(\frac{2\pi}{L}\frac{P}{P_0}\right). \tag{3.8}$$

The set of angles $\psi_l(1\leqq l\leqq L)$ obeying (3.4) (with $\psi_{l+nL}\equiv\psi_l+2\pi n$), (3.7) and (3.8) represents our

lattice bulk solution. The corresponding director values constitute the boundary conditions on the bottom row of the two-dimensional-lattice calculations of the following sections.

3.3. *Structure of the director field*

There have been suggestions that the director field in the fingerprint texture of a sample with homeotropically aligning substrates in a perpendicular magnetic field can adapt to the boundary conditions without producing disclination lines with singularities in the director field n. A quite convincible proposal was advanced by Press and Arrott [4, 5]. We have utilized their topology of the surface structure in the following calculations. Figure 1 shows a pictorial view of this structure as calculated in a 32×32 lattice model. This structure shows a periodicity of a full pitch P while other proposed structures with half integral disclination lines [3] show a shorter period of $P/2$. Our observations of samples show clearly a periodicity of P, which led us to favour Press and Arrott's proposal. In particular, in high applied fields the now metastable cholesteric lines display large homeotropic regions between each other. However, the width and structure of the lines correspond to a full 2π-turn of the director, showing that P rather than $P/2$ in the unit of the cholesteric structure between homeotropically orienting substrates (see also [4]). Furthermore our minimization procedure has never led away from this basic structure.

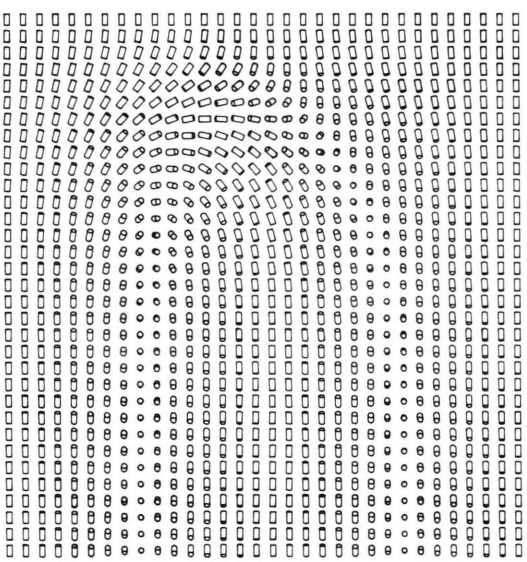

Fig. 1. Lattice picture of the configuration of the nematic director in a surface structure of the type considered in this work. The top and bottom row are held fixed to provide homeotropic boundary conditions and the bulk configuration respectivley. The rows in between are subjected to a minimization procedure for the free energy (3.1 and 3.2). The periodicity corresponds to the lattice solution in the given applied magnetic field which is here $h = 0.672$ (3.9). The pitch value in zero field is 0.959 times the period. Other parameter values were $\sigma = \tau = 0$. This lattice is called a quadratic 32×32 lattice even though it contains 33 rows. Such singularity-free configurations have been proposed in [4].

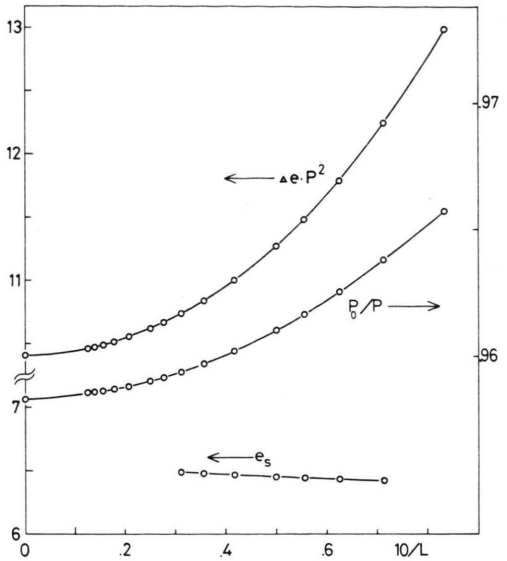

Fig. 2. Size dependence of various quantities. The top graphs show $\Delta e\, P^2$ (3.10) and P_0/P as they approach the continuum limit with increasing number L of lattice points per period. The bottom graph shows the surface energy e_s (3.11) for a quadratic lattice. This central quantitiy varies only slowly with L. In these calculations $h\, P/P_0$ was kept fixed at a value of 0.7 thus givsng a slight L-dependence of h. Other parameters were $\sigma = \tau = 0$.

3.4. *Lattice size*

The calculation time for minimizing the free energy increases drastically with increasing size of the lattice. For this reason it is desirable to know to what degree of accuracy a finite lattice calculation approaches the results of the continuum description. Figure 2 shows various results obtained for a sequence of lattices of increasing size. It is evident that the energy increment over the bulk solution energy varies very little with the lattice size while the changes in the bulk energy are somewhat larger. Thus it appears that quite reliable values for the

surface energies can already be obtained from a lattice of only 16 sites per period P.

3.5. *Depth of the surface structure*

In order to obtain reliable energies for the surface structure, one has to be sure that the lattice extends far enough away from the surface, so that the imposed bulk solution on the bottom row does not influence the surface structure. For this reason calculations with a variable number of rows M (top row not counted) have been made for various values of the magnetic field

$$h \equiv q_H P_0/\pi^2 , \tag{3.9}$$

h being the reduced field H/H_c in the continuum limit.

The results of Fig. 3 show that the surface energy stays constant as soon as L/M becomes smaller than 0.7 for $0.4 \leqq h \leqq 0.99$. For values $h \leqq 0.2$ the surface structure extends farther into the bulk than 1.5 times the pitch. This is probably caused by the fact that in zero field a Grandjean-type structure is most compatible with the homeotropic boundary conditions [11]. Correspondingly, in small fields fairly extended regions near the surface show already a structure in which the helix axis tends to rotate out of the substrate plane. This may be interpreted as a step towards the Grandjean structure. This behaviour is illustrated in Fig. 4, which shows the configuration as obtained from a minimization calculation.

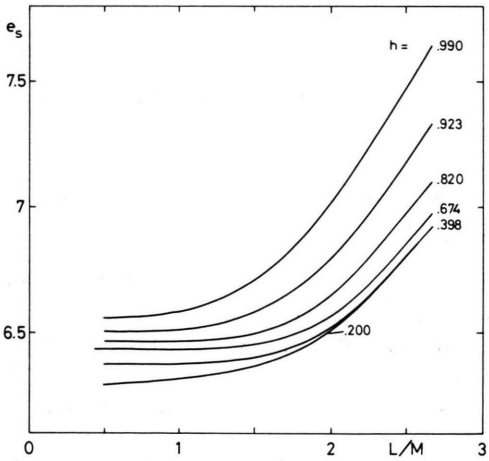

Fig. 3. Dependence of the surface energy e_s (3.11) on the aspect ratio $r = L/M$ of the lattice for various values of h. It is seen that for values of h around 0.7 the result of the bulk row-solution is reached nearest to the surface (e_s stays constant to largest values of r). For higher as well as for lower fields this distance increases. In these calculations the parameters were $\sigma = \tau = 0$, $L = 16$.

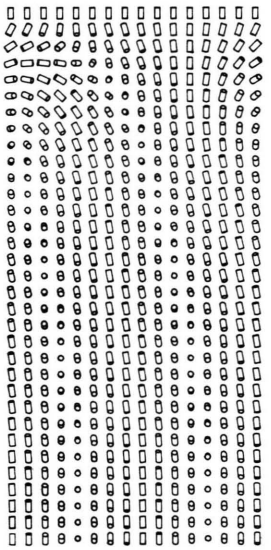

Fig. 4. Illustration of the tilt of the helical axes near the surface for low values of the magnetic field (here $h = 0.2$). In this 16×32 lattice the imposed bulk configuration of the bottom row still enforces a non-natural solution (compare Figure 3). The center of the surface structure has been shifted to the left owing to the tilt of the helical axis. Parameters were $\sigma = \tau = 0$.

3.6. *Magnetic field dependence*

The magnetic field dependence of the lattice model energy is shown in Figure 5. The smaller the number of lattice points per period the larger is the increase in the energy difference

$$\Delta e \equiv L P^{-2} \sum_{l=1}^{L} (F_{l,\,\text{homeotropic}} - F_{l,\,\text{bulk}})\, a^2/k_{22} \tag{3.10}$$

over the continuum solution. This leads on the one hand to an enhanced value for the critical field $H_{c,L}$ compared to the continuum value H_c (2.3). $H_{c,L}$ is determined by the condition $\Delta e = 0$. On the other hand a quite pronounced (especially for low L) levelling of the finite lattice curves $\Delta e(h)$ appears as soon as h is near or above one. This indicates that conclusions drawn from the lattice model calculations must be based on results obtained for h smaller than one in order to be generalizable to the continuum limit.

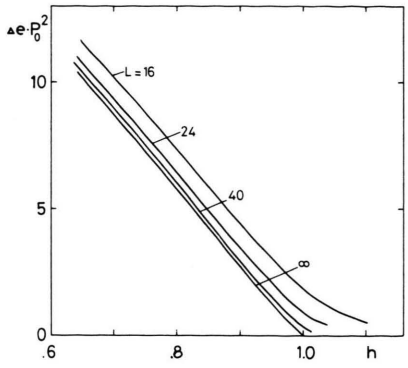

Fig. 5. Difference between the energies of the homeotropic state and the bulk solution $\Delta\varepsilon$ (3.10) multiplied by P_0^2 for values of h near one. For h-values below one the curves for different number of lattice sites L per period lie roughly parallel to the continuum graph. For h-values close to or above one the deviations become larger. With decreasing L these deviations appear over an increasing range of h-values. In this region the lattice-model results are expected to give rather unreliable estimates for the continuum-model quantities.

Furthermore, regarding the surface energy calculations it must be taken into account that for small Δe our surface structure induces an alternating dilation and contraction in the almost homeotropic regions of the bulk solution. This alternation vanishes only with a fairly large extrapolation length away from the substrate. Figure 6 shows the surface energies obtained for two lattices of different size as a function of h. Both graphs exhibit a fairly weak dependence on h with the indication of some increase for $h > 0.9$. Ignoring this increase, the calculation yields a value of

$$e_s = \sum_l (F_l - F_{l,\text{bulk}})\, a^2/k_{22} \approx 6.45, \quad \sigma = \tau = 0 \qquad (3.11)$$

for the energy of a single surface structure taken per unit length.

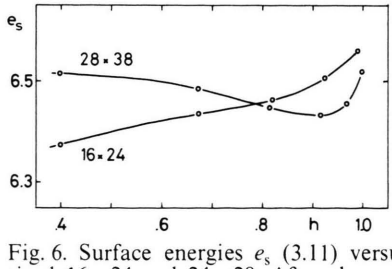

Fig. 6. Surface energies e_s (3.11) versus h for lattices of sized 16×24 and 24×28. After slow variation for low h-values there seems to be the indication on an increase near $h = 1$. However, in this region the lattice approximation may lead to large deviations from the continuum solution as apparent in Figure 5. Parameters were $\sigma = \tau = 0$.

Table 1. Energies of surface structures per unit length e_s in units of k_{22} (3.11) for various values of the parameters σ and τ (Eq. (2.8)) as obtained from the lattice model (3.1). The results were obtained from a lattice with a period of 16 sites and a depth of 24 sites. The reduced magnetic field was $h = 0.923$.

σ \ τ	0	0.5	1.0	1.5	2.0
0	6.51	7.58	8.48	9.07	9.34
0.5	7.30	8.39	9.36	10.25	11.05
1.0	7.95	9.07	10.07	10.99	11.86
1.5	8.53	9.67	10.68	11.61	12.47

3.7. *Elastic-constant dependence of surface energies*

Compared to the case $\sigma = \tau = 0$ the calculations become increasingly elaborate for $\sigma \neq 0$ and even more so for $\tau \neq 0$. For this reason we have restricted the calculation of e_s in these cases to a single value of $h = 0.923$ and to a lattice of size $L = 16$, $M = 24$. The results are shown in Table 1. The range of parameter values σ and τ has been chosen such that it includes the experimentally accessible values as well as the theoretically most simple case $\sigma = \tau = 0$ which appears not to be favoured by nature. The values of e_s increase with increasing σ and somewhat stronger with increasing τ. Their values span a range of roughly a factor of two when (σ, τ) change from $(0, 0)$ to $(1.5, 2)$ It is tempting to try to describe the observed dependence by relatively simple expressions in σ and τ. A description which appeared rather satisfactory to us was

$$e_s \approx A\,[(1+\sigma)^{\alpha} \cdot (1+\tau)^{1-\alpha}]^{\beta} \qquad (3.12)$$

which from the data of Table 1 yields the least square fit values

$$\begin{aligned} A &= 6.52 \pm 0.05\,, \\ \alpha &= 0.437 \pm 0.009\,, \\ \beta &= 0.637 \pm 0.012\,. \end{aligned} \qquad (3.13)$$

The expression (3.12) then reproduces the values of Table 1 with an average deviation of 0.12.

This is illustrated in Fig. 7 which shows a plot of calculated e_s-values versus $(1+\sigma)^{\alpha\beta}(1+\tau)^{(1-\alpha)\beta}$. An interesting feature of (3.12) is the dependence on the *single* variable

$$\varrho = (1+\sigma)^{\alpha}(1+\tau)^{1-\alpha} \qquad (3.14)$$

which is some weithted logarithmic average of the ratios k_{11}/k_{22} and k_{33}/k_{22}.

The simplicity of this scaling variable is quite surprising.

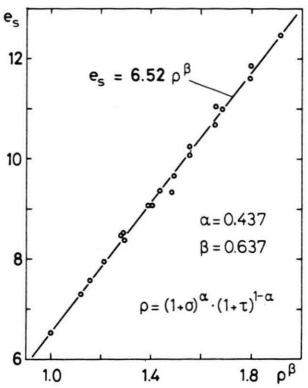

Fig. 7. Plot of the calculated surface energies e_s (3.11) versus ϱ^β where ϱ is the scaling variable composed of the elastic constant ratios k_{11}/k_{22} and k_{33}/k_{22} (3.14). The power law (3.14) is fullfilled fairly accurately. All calculated values were obtained from a 16×24 lattice with a value of $h = 0.923$.

4. Conclusion and Comparison with Experiments

We have seen in Sect. 2 that the cholesteric-nematic threshold field H_γ for a sample of thickness, d, with homeotropic boundary conditions, decreases linearly with P_0/d from the bulk value H_c (2.3). This dominant behaviour may possibly be modified by logarithmic correction terms (2.13). Neither from the numerical work of Sect. 3 nor from the experiments discussed below a decision appears possible regarding the presence of these terms. However, the numerical calculation gives values for the surface contributions to the energy which appear to vary little in the h-range easily accessible by the experiment. Thus in this pre-asymptotic range a comparison of experiment and numerial work is certainly meaningful. Our previous experimental results [11] were obtained with a cholesteric substance having the following parameters:

$$\sigma_1 = 0.76, \quad \tau_1 = 1.76 . \tag{4.1}$$

They yielded for the coefficient B of the threshold voltage expression (compare 2.13):

$$1 - V_{ch,n}(d)/V_{ch,n}(\infty) \approx B P_0/d \tag{4.2}$$

an experimental value of

$$B_1 = 0.77 \pm 0.05 . \tag{4.3}$$

In order to enlarge the range of parameter values we have added a measurement with a substance having

$$\sigma_2 = 1.27 , \quad \tau_2 = 1.43 \tag{4.4}$$

for which the dielectric constants were

$$\varepsilon_\parallel = 8.72 \quad \text{and} \quad \varepsilon_\perp = 3.32 .$$

The measurement of $V_{ch,n}$ versus P_0/d obtained in these experiments are shown in Fig. 8 and yield the coefficient

$$B_2 = 0.76 \pm 0.05 . \tag{4.5}$$

The details of this experiment were as described earlier in [11].

These numbers B_1 and B_2 may be compared with the expression

$$B = \left(\frac{1}{2\pi^2}\right) e_s \tag{4.6}$$

obtained from (2.13), with the appropriate numerically obtained e_s-values. However, one has to keep in mind that in the experiments electrical fields have been applied. Due to the large dielectric anisotropies of the liquid crystals these fields are not constant but vary across the sample, in particular near the surface regions. This leads, most certainly, to somewhat modified values, e_s^{el}, when compared to our magnetic-field calculations for e_s, which imply a constant field all over the

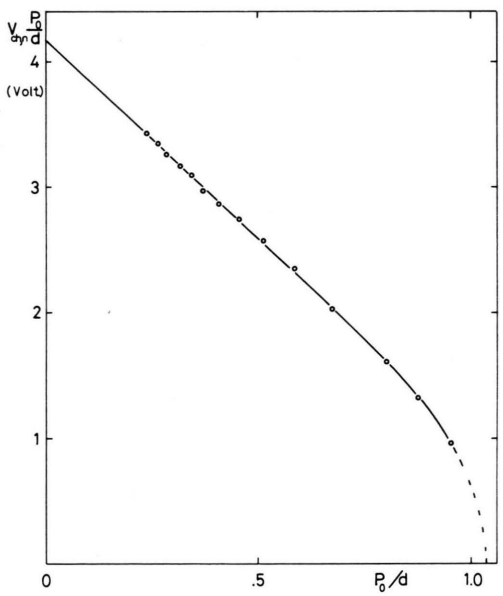

Fig. 8. Plot of experimental threshold voltages $V_{ch,n}$ multiplied by P_0/d versus P_0/d. The pitch of the cholesteric was $P_0 = 11.66\,\mu m$. The plotted points indicate a nice linear asymptotic behaviour as P_0/d goes to zero. Details of the experimental procedure are given in [11].

sample. Despite this difference, a comparison of experiments and calculations is of interest. From the values (4.1) and (4.4) one obtains $\varrho_1 = 2.27$ and $\varrho_2 = 2.36$ (Equation (3.14)). The similarity of these two values leads through (3.12) and (4.6) to the expectation of similar B-values in accordance with the experiment. The calculated values (though 4.1, 4.4, 3.12 and 4.6)

$$B_{1,\mathrm{calc}} = 0.56\,, \quad B_{2,\mathrm{calc}} = 0.57$$

are somewhat low compared to the experiments (4.3) and (4.5) but keep reasonably within the expectations considering the above mentioned arguments.

With respect to possible applications the knowledge of the dependence of the finite size modification of the critical field is useful for estimating the gap of metastability towards lower field values which is determined by Greubels threshold [7] voltage

$$V_G = \pi \frac{d}{P_0} \left\{ \frac{k_{22}}{\varepsilon_0 \Delta\varepsilon} \left[\frac{4}{1+\tau} - (1+\tau) \left(\frac{P_0}{d} \right)^2 \right] \right\}^{1/2}.$$

Depending on the particular requirements of a given application the values of σ and τ can be chosen optimally.

It is certainly desirable to continue this investigation along several lines. Firstly the case of homogeneously (in plane) aligning boundary conditions deserves a detailed investigation. In this case the loss of symmetry yields a richer variety of possibilities. Secondly, calculations with two surfaces present are of interest and thirdly the case of an applied electric voltage with its non-constant field distribution should be included. These questions must, however, be the subject of future investigations.

Acknowledgement

The author thanks Dr. M. Schadt for a critical reading of the manuscript.

[1] P. G. De Gennes, Solid State Comm. **6,** 163 (1968).
[2] R. B. Meyer, Appl. Phys. Lett. **12,** 281 (1968).
[3] P. E. Cladis and M. Kléman, Mol. Cryst. Liquid Cryst. **16,** 1 (1972).
[4] M. J. Press and A. S. Arrott, J. de Phys. **37,** 387 (1976).
[5] M. J. Press and A. S. Arrott, Mol. Cryst. Liquid Cryst. **37,** 81 (1976).
[6] D. L. White and G. N. Taylor, J. Appl. Phys. **45,** 4718 (1974).
[7] W. Greubel, Appl. Phys. Lett. **25,** 5 (1974).
[8] K. H. Walter and H. H. Krüger, B. Bunsenges. **78,** 912 (1974).
[9] M. Schadt and P. R. Gerber, Mol. Cryst. Liquid. Cryst. **65,** 241 (1981).
[10] P. G. De Gennes, The Physics of Liquid Crystals, Clarendon Press, Oxford 1974.
[11] P. R. Gerber, Z. Naturforsch. **36 a,** 718 (1981).